Original Research

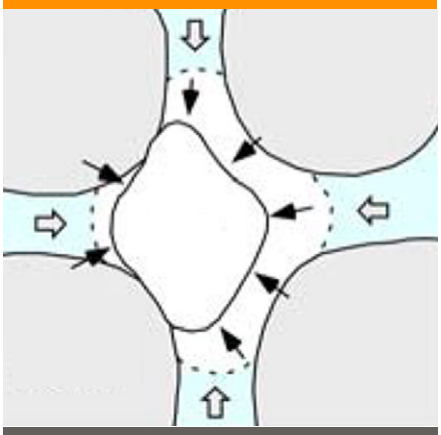

Core Ideas

- A quasi-saturated zone with trapped air was subjected to high water pressure.
- Saturation was measured using a dielectric soil moisture sensor.
- Saturation increase due to compression of air was well described by Boyle's law.
- The water retention curve was extended to the positive water pressure domain.
- We propose a mathematical model for the water retention curve in the extended domain.

T. Sakaki, International Services and Projects Division, National Cooperative for the Disposal of Radioactive Waste (Nagra), Wettingen, Switzerland; M. Komatsu, Graduate School of Environmental and Life Science, Okayama Univ., Okayama, Japan; and R. Takeuchi, Japan Atomic Energy Agency (JAEA), Tono Geoscience Center, Gifu, Japan. *Corresponding author (Toshihiro.Sakaki@nagra.ch).

Vadose Zone J.
doi:10.2136/vzj2015.12.0165
Received 17 Dec. 2015.
Accepted 20 May 2016.
Open access

Vol. 15, Iss. 8, 2016

Extending Water Retention Curves to a Quasi-Saturated Zone Subjected to a High Water Pressure up to 1.5 Megapascals

Toshihiro Sakaki,* Mitsuru Komatsu, and Ryuji Takeuchi

On closure of an underground facility, recovery of the geoenvironmental conditions is one of the essential issues for ensuring proper implementation of closure. At the Mizunami Underground Research Laboratory, Gifu, Japan, a tunnel flooding test is underway in which a section of a deep underground tunnel is filled with groundwater and the existing desaturated zone with trapped air is subjected to high water pressure. Water saturation in the unsaturated zone as a function of capillary pressure is well understood. However, the process of a saturation increase due to a further increase in water pressure is less well studied. In this study, a simplified laboratory setup using test sands with trapped air was established in a pressure chamber. The relationship between the positive water pressure up to 1.5 MPa and saturation was measured and the effect of the compression of trapped air bubbles on the change in saturation was investigated. The experimental results showed that the saturation increased further from the initial saturation of about 0.85 at zero suction. Most of the saturation increase occurred up to a water pressure of 0.5 MPa, at which the saturation reached 0.98. At 1.5 MPa, the air bubbles were compressed to a non-detectable level so that the sands were fully saturated. A mathematical model was established based solely on Boyle's law to define the water retention curve in a broad sense for the domain where the water pressure is positive. The measured water pressure–saturation data closely followed the relationship estimated with the established model.

Abbreviations: WRC, water retention curve.

On completion of the operational phase of underground openings such as mines and tunnels, the openings are often subjected to closure. At the Mizunami Underground Research Laboratory, Gifu, Japan, a tunnel flooding test is underway with the scientific goal of investigating the impacts of closure of an underground opening on the geoenvironmental recovery processes. A section of a tunnel located 500 m below the ground surface with a length of 46.5 m, width of 5 m, height of 4.5 m, and isolated with a concrete plug was flooded with groundwater, and various parameters such as water pressure, water content, and water chemistry are monitored. The test tunnel section has been exposed to atmospheric conditions with ventilation for about 2 yr since February 2014 and part of the near-wall zone, including the lining and excavation damaged zone, is thus expected to be unsaturated (Onoe et al., 2014). During the flooding test, the unsaturated zone first comes into direct contact with groundwater and is subjected to resaturation. The water pressure had risen to 3.1 MPa as of February 2016. During the early phase, rapid flooding may not allow the air in the unsaturated zone to escape, leading to trapped air remaining in discrete form in the voids. The behavior of the trapped air with the rise in water pressure (P_w) during flooding can control the flow in the rock around the tunnel. Thus, it is important that this behavior is understood properly to better assess the impact of resaturation on geoenvironmental recovery processes as a result of, e.g., underground facility closure.

The unsaturated zone with an isolated or disconnected trapped air phase is referred to as the "quasi-saturated" zone (Faybishenko, 1995; Sakaguchi et al., 2005). Christiansen (1944) showed experimentally that trapped air in soils resulted in a significant reduction in the permeability, the degree of which was affected by the dissolution of air into water, water pressure, and temperature. Findings in the literature on the effect of trapped air on permeability were summarized by Faybishenko (1995). The large effect of trapped air on permeability can also be inferred from the strong dependence of relative permeability on saturation in the high saturation range, such as in the model of Brooks and Corey (1964).

The water retention curve (WRC) is another crucial constitutive relationship that describes the relationship between the capillary pressure (P_c) and saturation (S). By conventional definition, the unsaturated zone exists above the groundwater table. Consequently, the WRC is defined for the region above the groundwater table where $P_c > 0$ (i.e., $P_w < 0$) as shown in Fig. 1, where P_c is defined as the difference between the air and water pressures, $P_a - P_w$. Note here that P_a is often assumed to be atmospheric ($P_a = 0$ gauge) and, thus, P_c is practically $-P_w$.

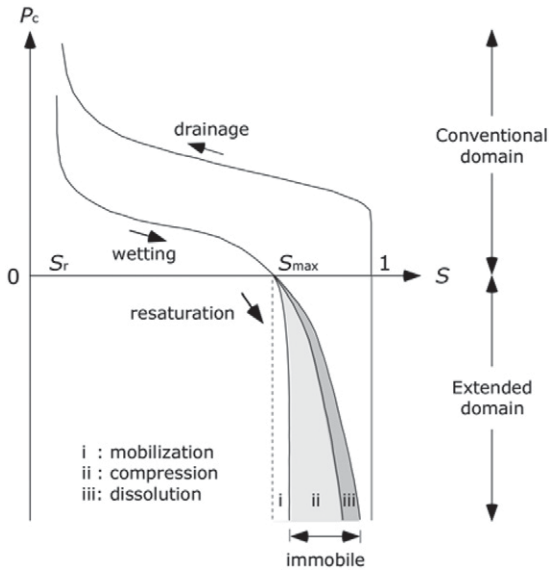

Fig. 1. Water retention curves in the conventional and extended domains. In the extended domain, contributions from three mechanisms (mobilization of mobile bubbles, compression and dissolution of immobile bubbles) are shown schematically.

Typical WRCs such as the one shown in Fig. 1 defined above the groundwater table indicate that S reaches the field maximum saturation S_{max} when P_c becomes zero at the end of the wetting cycle. Below the water table, on the other hand, air can exist in the form of entrapped air bubbles (e.g., Peck, 1960). Inside the bubble, a pressure is generated due to interfacial tension to resist the external water pressure. There is, however, no established method for measuring such internal pressure in small air bubbles (Corey and Brooks, 1997). Even if P_a in air bubbles was measured, as described below, calculations have shown that the effect of the internal air pressure becomes significant only when the trapped bubble diameter is extremely small.

Trapped air can be divided into mobile and immobile bubbles (Faybishenko, 1995). When P_w increases in the quasi-saturated zone, it is expected that S will increase via three major mechanisms, as illustrated in Fig. 2: (i) movement of mobile air bubbles, (ii) compression of immobile air bubbles (as controlled by Boyle's law, e.g., Fredlund, 1976), and (iii) dissolution of immobile air into water (as controlled by Henry's law, e.g., Fredlund, 1976).

During the early phase of the resaturation process in the quasi-saturated zone, due to a rise in water pressure, the mobile air bubbles become mobilized and contribute to the increase in S. The immobile air bubbles, on the other hand, are subjected to compression and dissolution under a further water pressure rise. These are depicted schematically in the bottom part of Fig. 1. The compression and dissolution behavior of the immobile trapped air bubbles in soils were studied, based on Boyle's law and Henry's law, to evaluate the density and compressibility of an air–water mixture (Fredlund, 1976) and to achieve full saturation of soil samples to obtain the saturated hydraulic conductivity by applying a backpressure (Black and Lee, 1973; Kohno and Nishigaki, 1982). According to Henry's law, the volume of air that dissolves in water is on the order of 2% of the volume of the water. On a short time scale, compression of air bubbles would probably control the volumetric changes in the air phase in the pore, whereas, on a longer time scale, the dissolution of air into groundwater could become more pronounced (e.g., Christiansen, 1944).

Despite the previous works mentioned above, little evidence is available on how the WRC is affected by the increase in water pressure in the quasi-saturated zone. This is partly because the need for a thorough understanding of saturation in soils with trapped air under high water pressure was not realized in typical

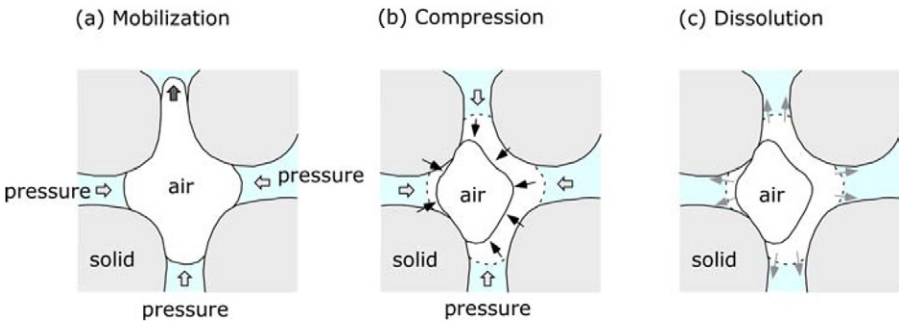

Fig. 2. Dominant mechanisms for saturation changes during the resaturation process: (a) mobilization of mobile bubbles, and (b) compression and (c) dissolution of immobile bubbles.

hydrological, agricultural, and environmental applications. This issue was raised in relation to geoenvironmental recovery during and after the resaturation of a deep underground facility, e.g., as being studied in the tunnel flooding test at the Mizunami Underground Research Laboratory (Onoe et al., 2014) described above. It may also be attributed to technical aspects—for example, that there is no method for measuring air pressure in small bubbles, as pointed out by Corey and Brooks (1997).

In this study, we extended the P_c–S curve to the domain where the water pressure is positive (in compression) as in Fig. 1 and considered as part of the WRC in a broad sense. Note here that S in the quasi-saturated zone is still defined as the volume fraction of the water phase in the pore, and the pressure in the air bubbles is ignored. Therefore, P_c still equals $-P_w$, which is identical to the definition in the conventional domain, and the P_c–S curve in the conventional domain continues to the extended domain as illustrated in Fig. 1. We specifically refer to the process where S in the quasi-saturated zone increases under positive water pressure as the *resaturation* process to distinguish it from the *wetting* process in the conventional domain where the pore water is under suction.

With the goal of generating experimental evidence for the WRC in the quasi-saturated zone under high positive water pressure up to about 1.5 MPa, a set of laboratory experiments was performed. Simplified conditions with the main focus on investigating the effect of the compression of immobile air bubbles trapped in permeable sands were adopted. A simple mathematical model describing the WRC in the extended domain with the effect of air bubble compression was established and compared with the measured data.

Materials and Methods

Experimental Setup

In this study, a pressure-resistant experimental setup as shown in Fig. 3 was developed. The pressure chamber (Swagelok, double-ended sample cylinder, 304L-HDF8-1000, maximum pressure of 12.4 MPa, nominal volume of 1 L) was equipped with a soil moisture sensor (EC-5, Decagon Devices) at the bottom for measuring saturation in the test sand. The cable of the EC-5 sensor was fed through a customized fitting and connected to a datalogger.

A ceramic porous cup (length 2.9 cm, diameter 6.4 mm) attached to a small tube was also placed at the bottom, as shown in Fig. 3. This was used to drain pore water and create unsaturated or quasi-saturated conditions in the sand as described in more detail below. At the top boundary of the pressure chamber, a pressure transducer, pressure relief valve, and a compressed air cylinder were installed. For the test sands, three uniform silica sands with

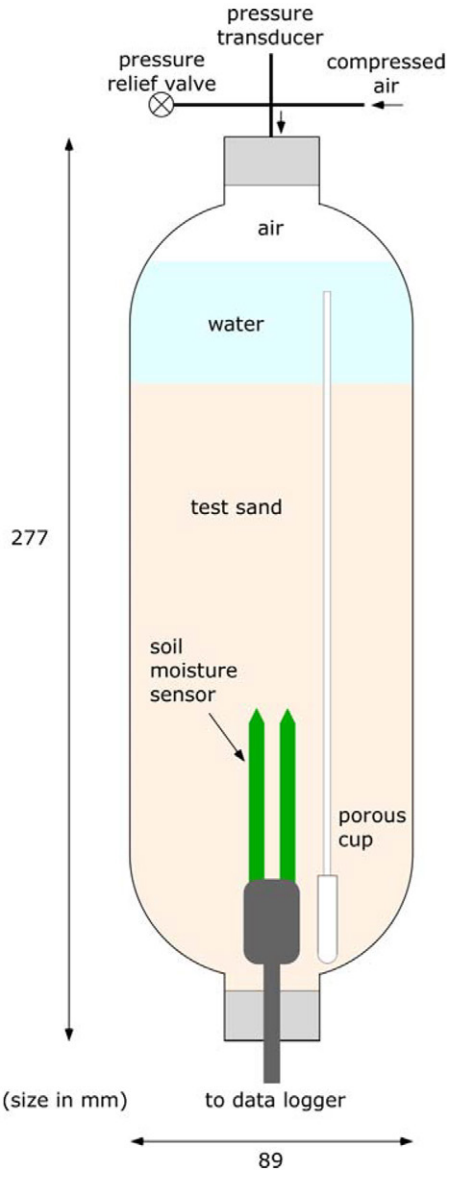

Fig. 3. Pressure chamber setup.

different particle sizes were used. The particle shape is classified as round. Selected properties of the test sands are provided in Table 1. The pore size in the in situ desaturated rock mass around an underground opening could be smaller in finer materials than the test sands, or larger in fractures, for example. The test sands with a particle size range of 0.1 to 1.0 mm cover most of the range of the sand category, and their physical and hydraulic properties are well characterized (e.g., Sakaki and Illangasekare, 2007; Sakaki et al., 2013a, 2013b).

Experimental Procedure

Moisture Sensor Performance under High Positive Water Pressure

Typical soil moisture sensors are designed for use in the unsaturated zone where the water pressure is generally negative (in suction) and the positive water pressure to be encountered in the resaturation

Table 1. Selected properties of the test sands.

Sand	d_{50}†	U_c‡	Dry density§	Porosity§	Saturated hydraulic conductivity, K_s§	Remark
	mm		Mg/m^3		cm/s	
A	1.04	1.2	1.81	0.32	0.38	Unimin Accusand no. 12/20
B	0.27	1.2	1.76	0.34	0.029	Unimin Accusand no. 50/70
C	0.12	1.7	1.76	0.33	0.0051	Ottawa Foundry sand, US Silica F-110

† d_{50}, median particle diameter.
‡ U_c, uniformity coefficient = d_{60}/d_{10}, where d_{10} and d_{60} are the particle sizes at which 10 and 60% (w/w), respectively, of a sample is finer.
§ Tightly packed, K_s is corrected to 20°C.

process, e.g., on closure of a deep underground facility, lies completely off the sensors' expected application range. Therefore, the selected EC-5 soil moisture sensor was first examined for its performance under high positive water pressure.

This test was needed to confirm that the sensor output is not affected by a high positive water pressure. It ensures that the readings in the experiments with the test sands reflect solely the saturation changes in the test sands. The EC-5 sensor was placed in the pressure chamber, and the chamber was filled with water. The water pressure was then increased up to 2 MPa in steps with intervals of 0.5 MPa. At each level, the water pressure was maintained for 5 min and the sensor readings in millivolts were taken every 10 s.

Acquisition of Capillary Pressure–Saturation Data

Three experiments were performed using the test sands described in Table 1. The moisture sensor was connected to a Campbell Scientific CR10X datalogger with an excitation voltage of 2.5 V. The sensor readings were in millivolts. The EC-5 sensor was calibrated using a two-point α mixing model (Sakaki et al., 2008, 2011). This model requires two sensor readings under dry and saturated conditions and one sensor type-specific fitting parameter, identified as 2.5 for the EC-5 sensor by Sakaki et al. (2008, 2011). See also the Results and Discussion section for the calibration equation. Each of the three tests was conducted as follows:

1. Dry packing: This step was done to obtain a moisture sensor reading (X_{dry}) in a dry condition for calibration (Sakaki et al., 2008, 2011). The chamber was first filled with dry sand. One of the test sands was poured and compacted by tapping the container wall to reach a porosity as shown in Table 1, a sensor reading (X_{dry}) was taken, and the sand was removed.

2. Wet packing: This step was done to obtain a moisture sensor reading (X_{sat}) in a saturated condition for calibration (Sakaki et al., 2008, 2011). The chamber was half-filled with water and the sand was poured in steps and compacted by tapping the container wall to reach a porosity as shown in Table 1. The level of water in the chamber was always kept above the surface of the sand to make sure that the sand was fully saturated with water. After compacting the sand to the porosity shown in Table 1, another sensor reading (X_{sat}) was taken.

3. Drainage of pore water (primary drainage process): The tubing of the ceramic porous cup was fed out of the top opening of the chamber and set at a low positon to induce slow drainage. The height of the tip of the tubing was set sufficiently low (>1 m lower than the sand surface) so that the pore water in the sand near the bottom drained and saturation reached residual saturation (S_r). This step was done to simulate the primary drainage process and to create a fully drained condition before wetting.

4. Wetting of sand (wetting process): The tubing was then connected to a Marriotte bottle and water was supplied to the sand. The height of the Marriotte bottle was set roughly 50 to 100 cm higher than the top surface of the sand. This height seemed to generate a gradual water supply through the porous ceramic cup. The Marriotte bottle was brought down to the height of the sand surface, and the water supply was terminated when free water started to accumulate on the surface of the sand. Some extra water was supplied on the surface so that the sand surface was covered by a layer of free water as in Fig. 3. This was assumed to be the end of the wetting process when the sand was quasi-saturated, with $S = S_{max}$ as defined in Fig. 1. This is the "initial" condition before starting the resaturation process.

5. Pressurization (resaturation process): The water supply tubing was rolled and placed inside the chamber, and the pressurizing unit was installed on the top opening. The pressure in the headspace of the chamber was gradually increased to 1.5 MPa by adjusting the pressure regulator on the compressed air cylinder. With the rate of pressure increase used (approximately 0.12 MPa/min), it took roughly 12 to 13 min to reach the maximum pressure. As the pressure increased, trapped air bubbles were compressed and more pore volume was occupied by water. The free water above the sand sample was maintained at more than what would go into the sand so that there was always a layer of free water. Due to the high permeability of the test sands, the flow of water took place sufficiently quickly to fill the volume that the air bubbles lost due to compression. During the pressurization, data from the pressure transducer and moisture sensor were recorded every 2 s.

6. Depressurization: After reaching the maximum pressure of 1.5 MPa, the pressure regulator was shut off. The pressure

relief needle-valve was opened slightly to slowly release the pressure. It took about 25 to 30 min until the pressure came down to atmospheric.

Steps 1–6 were repeated for the three test sands.

Mathematical Model for Compression-Controlled Capillary Pressure–Saturation Curve

As noted above, a bubble under water generates an internal pressure due to interfacial tension to resist the external water pressure. Figure 4 shows the volume reduction of a single air bubble under water due to compression. The volume reduction of the air bubble was calculated using Boyle's law (described below) with and without taking the effect of the internal bubble pressure into account. For cases where the internal bubble pressure was considered (with an interfacial tension of 0.071 N/m), four hypothetical media with particle diameters as shown in the figure were selected. For simplicity, the initial diameter of the air bubble in each medium was assumed to be 30% of the particle diameter, which equals the mean pore diameter (e.g., Takahashi et al., 2008). It was observed that, for coarse to very fine sands, the curves coincided with the Boyle's law curve without the internal bubble pressure. This suggested that compression of air bubbles of this size showed negligible effects of the internal bubble pressure. On the other hand, the curve for a medium with the particle size of silt indicated that a bubble of this size started showing some effects of the internal bubble pressure on its volumetric change, which was more pronounced for a medium with the particle size of clay. We concluded that the effects of the internal bubble pressure would be insignificant unless the bubble diameter was extremely small, i.e., in the order of 1 μm, which was not the case for the test sands used in this study.

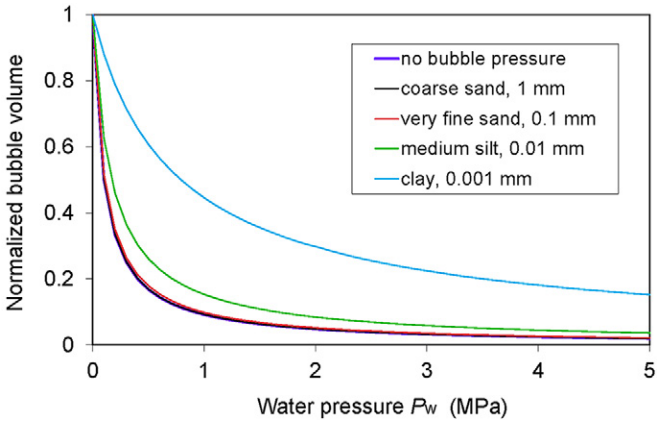

Fig. 4. Volumetric change in air bubbles with different diameters based on Boyle's law with and without the effect of internal bubble pressure. The initial bubble diameter at zero water pressure was assumed to be 30% of the particle diameter of the materials shown.

The volume reduction of an air bubble calculated using Boyle's law without the internal bubble pressure in Fig. 4 was then used to estimate the saturation increase starting from the measured S_{max} values as follows. Boyle's law is defined as

$$P_1V_1 = P_2V_2 = \text{constant} \quad [1]$$

where P_1 and P_2 are gas pressures and V_1 and V_2 are gas volumes under P_1 and P_2, respectively.

In a medium with saturation of S_{max} under atmospheric pressure P_0 (= 101.3 kPa), the volume fraction of air is $1 - S_{max}$. At a certain depth with an additional water pressure P_w, the new pressure and volume fraction of air are $P_0 + P_w$ and $1 - S$, respectively, where S is the new saturation of interest. Substituting these into Eq. [1] yields

$$P_0(1-S_{max}) = (P_0 + P_w)(1-S) \quad [2]$$

Solving Eq. [2] for S gives

$$S = 1 - \frac{1-S_{max}}{1+P_w/P_0} \quad [3]$$

Equation [3] describes the changes in S with changes in P_w based on the assumptions that: (i) compression of immobile air bubbles can be fully described by Boyle's law with insignificant effects of internal air bubble pressure, and (ii) no air bubble movement and dissolution into water are considered. The validity of this model was evaluated with the experimental data for the three test sands.

Results and Discussion

Soil Moisture Sensor Performance under High Water Pressure

Figure 5 shows the sensor output values under varied water pressure conditions. The water pressure was increased and decreased

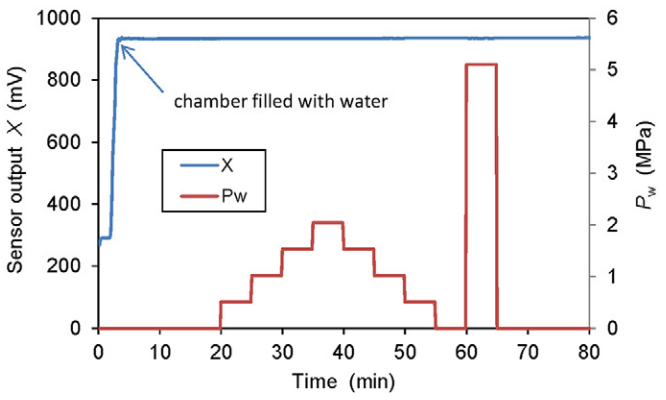

Fig. 5. Output values of the EC-5 soil moisture sensor under various water pressures P_w. No pressure dependence was observed.

at 0.5 MPa intervals up to 2 MPa in the first part of the test, and this was then followed by another one-step increase up to 5 MPa. For the range of water pressure P_w applied, the sensor output value X remained practically unchanged. Therefore, the data for the test sands shown below reflect solely the saturation behavior due to volumetric changes of the trapped air bubbles.

Capillary Pressure–Saturation Data under High Water Pressure

Figure 6 shows the P_c–S data for the resaturation process up to a water pressure of 1.5 MPa. Note again that $P_c = P_a - P_w$, where P_a (i.e., the internal bubble pressure) was ignored. The S values are those estimated by the two-point α mixing model $(X^{2.5} - X_{dry}{}^{2.5})/(X_{sat}{}^{2.5} - X_{dry}{}^{2.5})$, where X is the present measurement (in mV), X_{dry} and X_{sat} are the values obtained under dry and saturated conditions, respectively (see above), and 2.5 is the sensor type-specific fitting parameter obtained for the EC-5 sensor (Sakaki et al., 2008, 2011). At the beginning of the resaturation process ($P_c = 0$), the X values for the test sands A, B, and C resulted in S_{max} values of 0.84, 0.85, and 0.85, respectively.

The results showed that the saturation increase due to the increase in water pressure was significant for the first 0.5 MPa (equivalent to a depth of 50 m), where S reached 0.98. The theoretical analysis by Kohno and Nishigaki (1982) considering the effects of compression and dissolution showed that soils with S_{max} of 0.898 or higher will be fully saturated under a backpressure of 0.5 MPa. Our test sands had S_{max} of 0.84 to 0.85, and having S of 0.98 at 0.5 MPa under the compression-dominated conditions therefore seems to be a good agreement. A further water pressure increase up to 1.5 MPa (equivalent to a depth of 150 m) led to the air bubbles being compressed to a nondetectable level so that the test sands were practically at full saturation (S = 0.99–1.0). For the three test sands with different particle sizes, no significant difference in the saturation change was observed. This was expected due to the insignificant effects of the internal bubble pressure presented in Fig. 4.

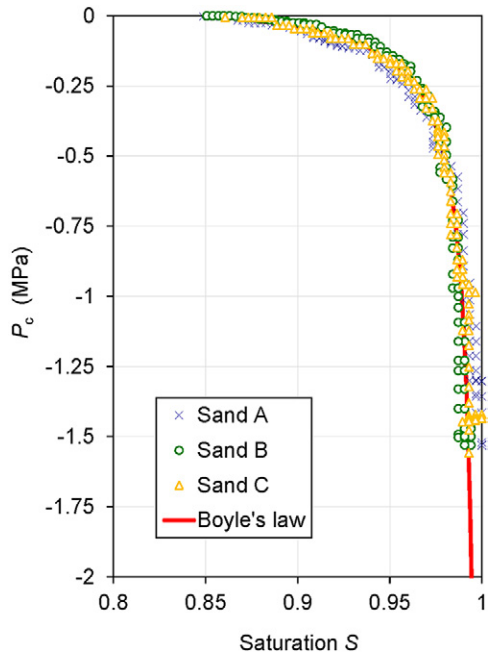

Fig. 6. Measured capillary pressure (P_c)–saturation (S) data for three test sands. The red line is the theoretical estimation with S_{max} = 0.85 based on Boyle's law without internal bubble pressure (Eq. [3]). The line coincides with the measured data.

The saturation increase due to an increase in water pressure estimated using Eq. [3] is also shown in Fig. 6. The resulting curve closely follows the experimental data for the three test sands. Boyle's law implies that the volume of air bubbles becomes one-half at a depth of 10 m under water, one-third at 20 m, one-fourth at 30 m, one-fifth at 40 m, one-sixth at 50 m, and so on, which can be inferred from Eq. [3]. For a material with S_{max} = 0.85, the air fraction in the pores is 15% at the beginning of the resaturation phase. At depths of 50 and 150 m, the air volume will be one-sixth and one-sixteenth of the initial volume, which leads to S = 0.975 and 0.991, respectively. This is consistent with the measured data as shown in Fig. 6. At a depth of 500 m where the tunnel flooding test is underway at the Mizunami Underground Research Laboratory, the volume of trapped air could reduce to 1/51 of the original volume, which leads to S = 0.997 if the water pressure reaches 5 MPa. In reality, such a small volume of air would dissolve into the groundwater with time, and saturation would thus reach 1.0.

Conclusions

Using three quasi-saturated test sands with zero water pressure created in a pressure chamber, water pressure was increased from zero up to 1.5 MPa (equivalent to a depth of 150 m) to simulate the resaturation process due to rapid water pressure recovery. The experimental results led to the following findings:

- Starting from S_{max} of 0.84 to 0.85 at zero water pressure, S further increased as the water pressure increased during the resaturation process. Most of the saturation increase occurred up to a water pressure of 0.5 MPa (equivalent to a depth of 50 m), at which S reached 0.98. At 1.5 MPa, S practically reached full saturation.

- Boyle's law without the effects of internal bubble pressure was incorporated into a mathematical model to define the P_c–S curve in the extended domain under high water pressure. The further increase in S from S_{max} observed in the experiments was well estimated based on the volume reduction of air bubbles due to compression.

- The P_c–S curve obtained in the resaturation process continues from the conventional wetting curve defined by typical parametric models (e.g., Brooks and Corey, 1964; van Genuchten, 1980). The P_c–S curve in the resaturation process as described, e.g., by the Boyle's law based model, can be plugged into

modeling tools as part of the constitutive relationships for cases where the water pressure in the unsaturated or quasi-saturated zone is expected to increase further into the positive side.

- Factors that were not considered in this study, such as the mobilization and dissolution of air bubbles, would further enhance the increase in *S*. These effects may become more pronounced for a slow resaturation rate and/or long-term resaturation process.

Acknowledgments

This research was partially funded by the Radioactive Waste Management Funding and Research Center, Japan. The sand samples were provided by the Center for Experimental Study of Subsurface Environmental Processes, Colorado School of Mines, Golden, CO. We are grateful to anonymous reviewers and the associate editor Markus Tuller of the University of Arizona for their helpful comments that improved this paper substantially.

References

Black, D.K., and K.L. Lee. 1973. Saturating laboratory samples by back pressure. J. Soil Mech. Found. Div., Am. Soc. Civ. Eng. 1:75–93.

Brooks, R.H. and A.T. Corey. 1964. Hydraulic properties of porous media. Hydrol. Pap. 3. Colorado State Univ., Fort Collins.

Christiansen, J.E. 1944. Effect of entrapped air upon the permeability of soils. Soil Sci. 58:355–366. doi:10.1097/00010694-194411000-00002

Corey, A.T., and R.H. Brooks. 1997. The Brooks–Corey relationships. In: M.Th. van Genuchten et al., editors, Proceedings of the International Workshop on Characterization and Measurement of the Hydraulic Properties of Unsaturated Porous Media, Riverside CA. 22–24 Oct. 1997. US Salinity Lab., Riverside, CA. p. 13–18.

Faybishenko, B.A. 1995. Hydraulic behavior of quasi-saturated soils in the presence of entrapped air: Laboratory experiments. Water Resour. Res. 31:2421–2435. doi:10.1029/95WR01654

Fredlund, D.G. 1976. Density and compressibility characteristics of air–water mixtures. Can. Geotech. J. 13:386–396. doi:10.1139/t76-040

Kohno, I., and M. Nishigaki. 1982. Some aspects of laboratory permeability test. (In Japanese.) J. Jpn. Soc. Soil Mech. Found. Eng. 22:509–518

Onoe, H., T. Iwatsuki, H. Saegusa, K. Ohnuki, R. Takeuchi, H. Sanada, M. Ishibashi, and T. Sato. 2014. Groundwater recovery experiment using an underground gallery in fractured crystalline rock. In: Proceeding of the 8th Asian Rock Mechanics Symposium, Sapporo, Japan. 14–16 Oct. 2014. Int. Soc. Rock Mech., Lisbon, Portugal.

Peck, A.J. 1960. The water table as affected by atmospheric pressure. J. Geophys. Res. 65:2383–2388. doi:10.1029/JZ065i008p02383

Sakaguchi, A., T. Nishimura, and M. Kato. 2005. The effect of entrapped air on the quasi-saturated soil hydraulic conductivity and comparison with the unsaturated hydraulic conductivity. Vadose Zone J. 4:139–144. doi:10.2113/4.1.139

Sakaki, T., and T.H. Illangasekare. 2007. Comparison of height-averaged and point-measured capillary pressure–saturation relations for sands using a modified Tempe cell. Water Resour. Res. 43:W12502. doi:10.1029/2006WR005814

Sakaki, T., A. Limsuwat, and T.H. Illangasekare. 2011. A simple method for calibrating dielectric soil moisture sensors: Laboratory validation in sands. Vadose Zone J. 10:526–531. doi:10.2136/vzj2010.0036

Sakaki, T., A. Limsuwat, K.M. Smits, and T.H. Illangasekare. 2008. Empirical two-point α-mixing model for calibrating the ECH$_2$O EC-5 soil moisture sensor in sands. Water Resour. Res. 44:W00D08. doi:10.1029/2008WR006870

Sakaki, T., M.R. Plampin, R. Pawar, M. Komatsu, and T.H. Illangasekare. 2013a. What controls carbon dioxide gas phase evolution in the subsurface? Experimental observations in a 4.5 m-long column under different heterogeneity conditions. Int. J. Greenhouse Gas Control 17:66–77. doi:10.1016/j.ijggc.2013.03.025

Sakaki, T., P.E. Schulte, A. Cihan, J.A. Christ, and T.H. Illangasekare. 2013b. Airflow pathway development as affected by soil moisture variability in heterogeneous soils. Vadose Zone J. 12(1). doi:10.2136/vzj2011.0118.

Takahashi, M., Y. Urushimaru, and H. Hirai. 2008. Challenge for quantification of pore structure in rock: An experimental approach to glass beads by micro focus X-ray CT. (In Japanese.) In: Proceedings of 12th Japan Symposium on Rock Mechanics, Ube, Japan. 2–4 Sept. 2008. Jpn. Committee for Rock Mech., Tokyo. p. 541–546.

van Genuchten, M.Th. 1980. A closed-form equation for predicting the hydraulic conductivity of unsaturated soils. Soil Sci. Soc. Am. J. 44:892–898. doi:10.2136/sssaj1980.03615995004400050002x